Interface Element Modeling of Fracture in Aggregate Composites

By Aleksander Zubelewicz[1] and Zdeněk P. Bažant,[2] Fellow, ASCE

Abstract: A brittle aggregate composite such as portland cement concrete or mortar is modeled in two dimensions as a system of perfectly rigid particles of various sizes separated by interface layers that are characterized by a given force-displacement relation for the normal and tangential components. The force-displacement relation exhibits for the normal component a tensile strength limit followed by a sudden drop of force to zero. The system of rigid particles is generated randomly. The particles are not allowed to overlap and are generally not in contact; however, when the distance between the particles is less than a certain limit, a deformable interface layer is introduced. Numerical simulation of a fracture specimen with a notch shows that the fracture front consists of an irregular band of interparticle cracks the width of which is about three maximum particle sizes. The interparticle cracks remain continuous and do not coalesce into a continuous line fracture until the deformation is very large. The load-displacement relation exhibits gradual softening after the peak force, with a rapid force decrease followed by a long tail of slowly decreasing force. These features qualitatively agree with observations of concrete.

Introduction

As transpired from recent researches, failure due to distributed damage such as cracking cannot be adequately modeled in a continuum manner using the usual, local continuum approach (Bažant 1986). This approach is incapable of describing the fact that the heterogeneity of the microstructure prevents the localization of damage into regions that are not sufficiently large compared to the inhomogeneity size. There are two ways to avoid this shortcoming: (1) Use a discrete rather than continuum model which directly simulates the microstructure; or (2) use a nonlocal continuum in which the continuum stress at a point depends not only on the strain at that same point but also on the strain distribution over a certain characteristic neighborhood of the point. While the latter approach, pursued in several recent works (Bažant and Oh 1983; Bažant et al. 1984; Bažant 1984; 1985; Bažant and Chang 1987), seems suitable for the analysis of large structures, the former approach, consisting of microstructure simulation, may reflect the material behavior more realistically. One type of such microstructural simulation will be presented in this study.

We will model concrete in two dimensions as a random arrangement of perfectly rigid particles separated by deformable interface layers that are characterized by force-displacement relations. This type of simulation of the behavior of concrete was recently proposed by Zubelewicz (1980) for the purpose of determining inelastic triaxial stress-strain relations, and was extended by Zubelewicz (1983) and Zubelewicz and Mróz (1983). In the present work, the idea is developed for concrete fracture. Our approach is similar to that previously formulated by Cundall (1971, 1978) and Cundall and Strack (1979) for loose granular solids such as sand, known as the distinct-element method. In Cundall's method, whose elementary idea had previously been suggested in the works of Serrano (1973) and Rodriguez-Ortiz (1974) and had also been independently introduced by Kawai (1980), the loose granular solid was modeled in two dimensions as a system of perfectly rigid circular discs (particles) which interact by contacts characterized by Coulomb friction law. In the present work, in which the concept is extended to concrete, the frictional interaction is replaced by a force-displacement relation with a tensile strength limit, and the rigid circular discs are replaced by rigid particles whose interfaces with the neighboring particles do not lie on a circle but on a polygon of arbitrary irregular shape. Random irregularity of the particle shape seems to be important for correct simulation of distributed cracking in a cementitious aggregate composite. Extension of Cundall's distinct-element method to the study of microstructure and crack-growth in geomaterials with finite interfacial tensile strength was previously proposed by Plesha and Aifantis (1983).

[1]Res. Sci., Ctr. for Concrete and Geomaterials, Northwestern Univ., Evanston, IL 60201.

[2]Prof. of Civ. Engrg., Northwestern Univ., Evanston, IL 60201.

Note. Discussion open until April 1, 1988. To extend the closing date one month, a written request must be filed with the ASCE Manager of Journals. The manuscript for this paper was submitted for review and possible publication on June 6, 1986. This paper is part of the *Journal of Engineering Mechanics*, Vol. 113, No. 11, November, 1987. ©ASCE, ISSN 0733-9399/87/0011-1619/$01.00. Paper No. 21921.

Two-Dimensional Mathematical Model

Concrete is a composite material consisting of hard inclusions—the aggregate pieces, embedded in a softer matrix—the mortar. We model the material as a system of perfectly rigid particles (elements) interacting at interface points according to a given force-displacement relation. Similarly to Cundall, we generate the system by starting with an array of N perfectly rigid circular discs of radii r^i ($i = 1,2, \ldots N$). These discs are randomly generated in such a manner that they can never overlap and do not have to contact any neighboring particle. Each particle is imagined to be surrounded by an annular influence zone of radius $R^i = \beta r^i$, where β = an empirical coefficient greater than one, chosen in the present simulation as $\beta = 1.2$. Many of such influence zones obviously intersect, and each straight-line interface connecting the two intersection points of the intersecting circular influence zones is characterized by a center point (Fig. 1). All the deformation of the interface layer of matrix (mortar) is supposed to be concentrated in the interface center and is described by a force-displacement relation. The set of interface centers defines straight-line interfaces which constitute the boundary of the rigid particle, simulating the hard aggregate pieces (Fig. 1).

The centers of the rigid particles (distinct elements) are characterized by cartesian coordinates x_i, y_i ($i = 1,2, \ldots$); see Fig. 1. The interface centers are numbered as $\nu = 1,2, \ldots n$, and the topological connectivity of the particle system is characterized by specifying an integer array that gives the number $n_c(i)$ of interfaces for each particle number i and another integer array that gives all the numbers $\nu(i,k)$ of the individual interfaces ($k = 1,2, \ldots n_c$) belonging to each particle number i. The arrays that give the numbers $i(\nu)$ and $j(\nu)$ of the two particles interacting at interface number ν are also generated. The interface centers are defined by their coordinates

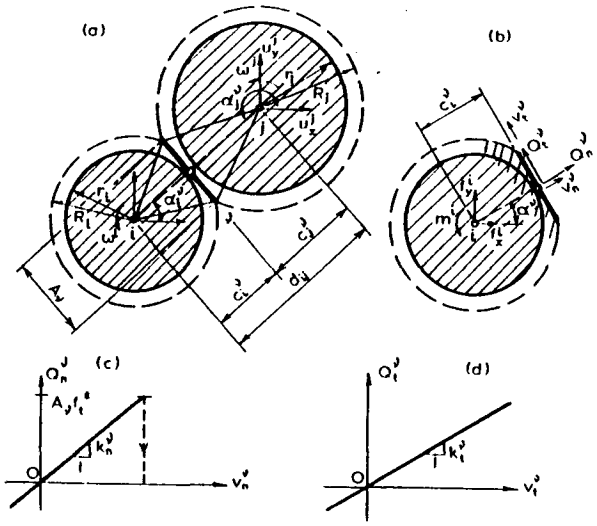

FIG. 1. (*a* and *b*) Rigid Particles (Distinct Elements) with Their Interface Centers and Interface Forces; (*c* and *d*) Diagrams of Interface (Interparticle) Forces versus Normal Displacements

x_ν, y_ν, and the orientation angle α_ν of the line connecting the centers of the two neighboring rigid particles (Fig. 1). Furthermore, the length A_ν of the line segment connecting the intersections of the two influence zone circles is thought to represent the effective interface area of the neighboring particles, and the distance h_ν between the adjacent circular discs is thought to represent the effective thickness of the interface zone of the matrix. The deformations in our simulation are assumed to be so small that the changes and rotations of the interface layer and of its thickness are negligible.

The displacement components u_x^i and u_y^i at the center of particle number i, the particle rotation ω^i, the components f_x^i and f_y^i of the force resultant through the particle center, and the resulting moment m^i about the particle center, may be arranged in column matrices as follows:

$$\mathbf{u}^i = \begin{Bmatrix} u_x^i \\ u_y^i \\ \omega^i \end{Bmatrix} = \begin{Bmatrix} U^{3i-2} \\ U^{3i-1} \\ U^{3i} \end{Bmatrix} \quad \text{..... (1a)}$$

$$\mathbf{f}^i = \begin{Bmatrix} f_x^i \\ f_y^i \\ m^i \end{Bmatrix} = \begin{Bmatrix} F^{3i-2} \\ F^{3i-1} \\ F^{3i} \end{Bmatrix} \quad \text{..... (1b)}$$

in which U^j and F^j ($j = 1,2, \ldots 3N$) represent the generalized displacements and force components in global numbering. The relative normal and tangential displacements at interface center number ν, and the tensile normal and tangential force components at this interface center, may be arranged in column matrices:

$$\mathbf{v}^\nu = \begin{Bmatrix} v_n^\nu \\ v_t^\nu \end{Bmatrix} \quad \text{..... (2a)}$$

$$\mathbf{Q}^\nu = \begin{Bmatrix} Q_n^\nu \\ Q_t^\nu \end{Bmatrix} \quad \text{..... (2b)}$$

The relative normal and tangential displacements v_n^ν, v_t^ν at interface center number ν (Fig. 1) may be expressed in terms of the displacements at the centers of adjacent particles number i and j as follows:

$$\begin{Bmatrix} v_n^\nu \\ v_t^\nu \end{Bmatrix} = \begin{bmatrix} \cos\alpha^\nu & \sin\alpha^\nu & 0 \\ -\sin\alpha^\nu & \cos\alpha^\nu & -c_j^\nu \end{bmatrix} \begin{Bmatrix} u_x^j \\ u_y^j \\ \omega^j \end{Bmatrix} - \begin{bmatrix} \cos\alpha^\nu & \sin\alpha^\nu & 0 \\ -\sin\alpha^\nu & \cos\alpha^\nu & c_i^\nu \end{bmatrix} \begin{Bmatrix} u_x^i \\ u_y^i \\ \omega^i \end{Bmatrix} \quad \text{..... (3)}$$

or $$v^\nu = -\mathbf{T}^{j\nu}\mathbf{u}^j - \mathbf{T}^{i\nu}\mathbf{u}^i \quad \text{..... (4)}$$

where $\alpha^\nu = \alpha_i^\nu = \alpha_j^\nu + \pi$ [Fig. 1(*a*)]; $\cos\alpha_i^\nu = -\cos\alpha_j^\nu$, $\sin\alpha_i^\nu = -\sin\alpha_j^\nu$; $\mathbf{T}^{i\nu}$ is a (2×3) transformation matrix between particle i and contact point ν, corresponding to angle ϕ_i^ν and radial distance c_i^ν. The force and moment resultants of all normal and tangential interface forces on particle number i may be calculated as

$$\mathbf{f}^i = \sum_{j=1}^{n} \mathbf{T}^{i\nu T}\mathbf{Q}^\nu \quad \text{..... (5)}$$

where superscript T denotes the matrix transpose. The interface center number ν is characterized by the force-displacement relation

$$\mathbf{Q}^\nu = \mathbf{k}^\nu \mathbf{u}^\nu \quad \text{..... (6a)}$$

$$\mathbf{k}^\nu = \begin{bmatrix} \phi_\nu k_n^\nu & 0 \\ 0 & k_t^\nu \end{bmatrix} \quad \text{..... (6b)}$$

in which $\mathbf{k}^\nu$ is the stiffness matrix for the contact layer; k_n^ν and k_t^ν are the normal and shear stiffnesses of the interface layer; and ϕ_ν is a cracking parameter. Initially its value is $\phi_\nu = 1$ (uncracked state), and after the tensile strength limit R_ν is reached [Fig. 1(*c*)], one may reset $\phi_\nu = 0$, assuming the normal force to drop suddenly.

The elastic normal and tangential stiffnesses characterizing the interface layer number ν may be assumed to be proportional to the interface area A^ν, i.e.

$$k_n^\nu = \frac{EA_\nu}{h_\nu} \quad \text{..... (7a)}$$

$$k_t^\nu = \frac{GA_\nu}{h_\nu} \quad \text{..... (7b)}$$

in which h^ν is the effective thickness of the interface layer; and E and G are material constants characterizing the elastic properties of the interface layer. The tensile strength of the interface layer must be also proportional to the effective interface area A^ν, i.e.

$$R_\nu = \phi_\nu A_\nu f_t^* \quad \text{..... (8)}$$

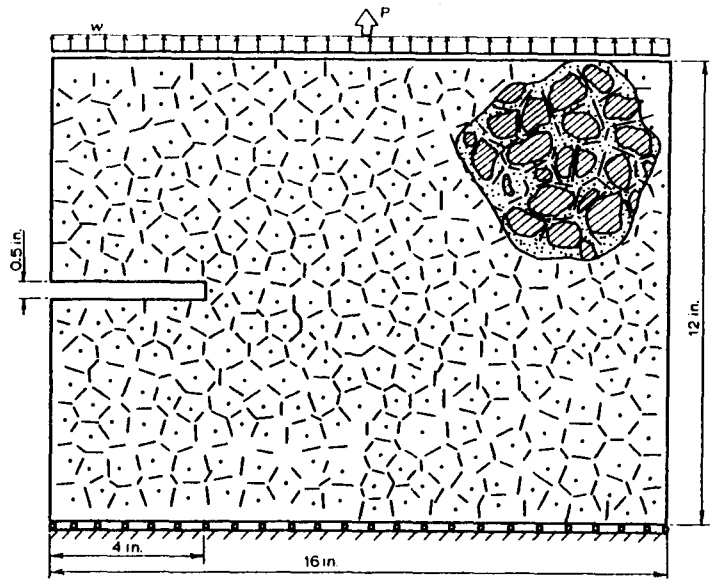

FIG. 2. Fracture Specimen Consisting of a Array of Rigid Particles and Their Interfaces

The equilibrium conditions of the rigid particle system, as shown in Fig. 2, require that $\mathbf{f}^i = 0$ for all $i = 1,2, \ldots N$. This generally represents a system of $3N$ algebraic equations for the displacements increments $\mathbf{u}_i$. This equation system is linear unless cracks are forming. The system has the form $\mathbf{K}\,\mathbf{U} = \mathbf{F}$ where $\mathbf{K}$ is the assembled global stiffness matrix of the system; and $\mathbf{F}$ are the forces associated with $\mathbf{U}$.

The boundary conditions are most easily implemented as the prescribed displacements or prescribed applied forces at the centers of the particles located at the boundary of the body. However, it is also possible to use the interface centers located at the boundary of the body and implement the boundary conditions as the prescribed displacements or the prescribed forces at these boundary interface centers.

The numerical solution is obtained by the secant method in a step-by-step incremental procedure. As long as no cracks are forming, the response of the particle system is linearly elastic, characterized by a linear load-displacement diagram through the origin, as shown by any of the dashed lines in Fig. 3(*a*). Since in our simple version of the interface element model we consider no inelastic phenomena other than tensile boundary cracking, the appearance of an interface crack merely causes a decrease in the elastic stiffness of the system. As long as no further cracks form, the system again behaves as linearly elastic, but with a load-displacement diagram whose slope gets smaller and smaller as further cracks form; see the sequence of dashed lines in Fig. 3(*a*). The response of the system to prescribed boundary displacements, characterized by a single displacement parameter w, may be calculated by the following algorithm:

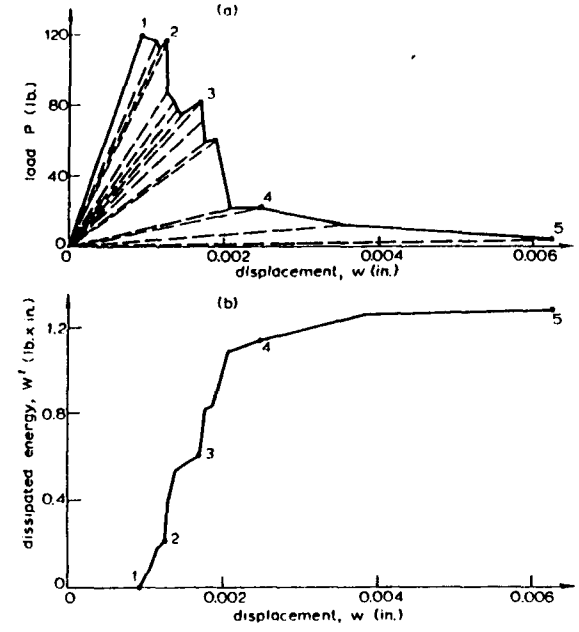

FIG. 3. (*a*) Load-Displacement Diagram for Fracture Specimen from Fig. 2; (*b*) Corresponding Diagram of Energy Dissipated by Fracturing

1. Initialize the cracking parameters for all interfaces ν as $\phi_\nu = 1$.

2. Calculate $\mathbf{k}^\nu$ and $\mathbf{T}^{i\nu}$ for all ν and i and assemble the elastic stiffness matrix $\mathbf{K}$ of the system. Then apply a unit boundary displacement $w = 1$ and solve the corresponding values $\overline{Q}_n^\nu$ of all normal interface forces Q_n^ν. Then determine the maximum value Y of the ratios $\overline{Q}_n^\nu/R_\nu$ ($\nu = 1,2, \ldots n$), and the value (or values) ν_c of ν at which this maximum occurs (or these maxima occur). The elastic solution for the current set of interface layer stiffnesses is then applicable up to the displacement value $w = 1/Y$. This corresponds to one of the dashed straight lines through the origin as shown in Fig. 3(*a*). At displacement $w = 1/Y$, this straight line terminates and cracks form at interface number $\nu = \nu_c$, after which a sudden stiffness reduction and a vertical drop of the applied force [shown by the vertical segments in Fig. 3(*a*)] is assumed.

3. For the interface center $\nu = \nu_c$, reset $\phi_\nu = 0$ and return to step 2, unless the specified final displacement has been exceeded.

The shear deformations at the interfaces are considered to be always elastic, characterized by the elastic interface shear stiffness k_t^ν (Eq. 6). This is certainly a simplification, since cracking also causes a reduction in the shear stiffness. However, the reduction might be quite small when the crack opening at the interface remains small, which should generally be true when the microcracks at the interfaces are discontinuous. Nevertheless, for large crack opening displacements u_n^ν, it would be more realistic to consider crack friction and dilatancy, in which case the interface

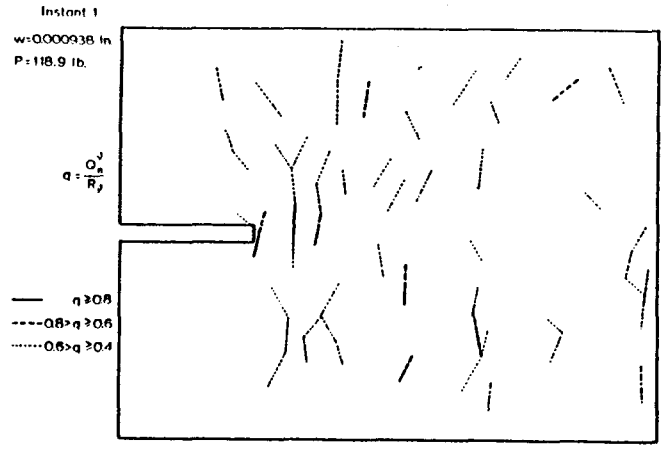

FIG. 4. Interparticle Forces and Interface Cracks in Specimen from Fig. 2 at First Instant of Loading, Corresponding to Point 1 on Load-Displacement Curve from Fig. 3(*a*) (Solid Lines-Forces Exceeding 80% of Strength Limit; Dashed Lines-60%; and Dotted Lines-40%)

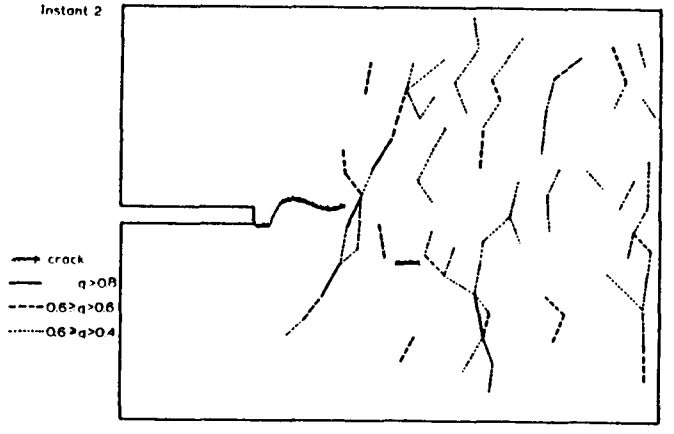

FIG. 5. Forces and Cracks as in Fig. 4 at Second Instant of Loading, Corresponding to Point 2 in Fig. 3(*a*)

stiffness matrix $\mathbf{k}^v$ (Eq. 4) would have nonzero off-diagonal terms and variable coefficients depending on u_n^v and u_t^v histories.

Numerical Simulation of Progressive Fracture

Consider the rectangular notched specimen shown in Fig. 2. The random array of particles, obtained from the circles the centers of which are marked by points, approximates the typical microstructure of concrete, as sketched in Fig. 2 according to a photograph of concrete cross section from

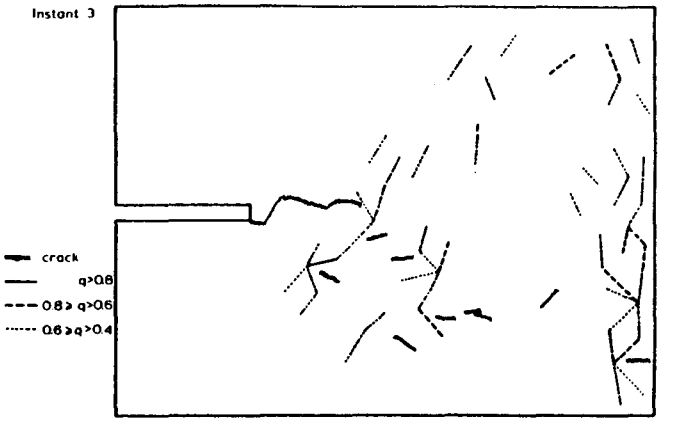

FIG. 6. Forces and Cracks as in Fig. 4 at Third Instant of Loading, Corresponding to Point 3 in Fig. 3(*a*)

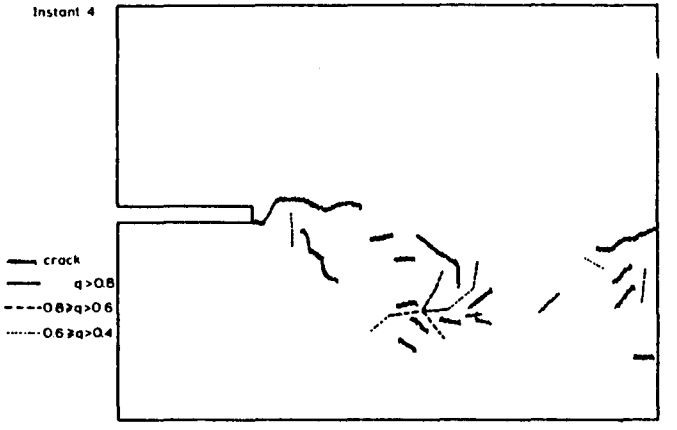

FIG. 7. Forces and Cracks as in Fig. 4 at Fourth Instant of Loading, Corresponding to Point 4 in Fig. 3(*a*)

Palaniswamy and Shah (1975). The specimen is fixed in the normal direction at its bottom boundary while its lateral deformations are uninhibited, and it is subjected at the top boundary to a uniform vertical upward displacement w.

The fracture specimen, shown in Fig. 2, consists of 264 particles, of which 84 are defined by circles of diameter not greater than 0.8 in., 148 not greater than 1.2 in., and 32 not greater than 1.6 in. (1 in. = 25.4 mm). The corresponding volumes of all the particles of each size are 0.055, 0.218, and 0.084 of the total specimen volume, respectively, the rest being the mortar. The influence zone parameter is chosen as $\beta = R_i/r_i$ = constant = 1.2. The elastic Young's and shear moduli of mortar in the interface layers (Eq. 6) are $E = 2.84 \times 10^6$ psi, and $G = 1.42 \times 10^6$ psi. The strength of mortar in

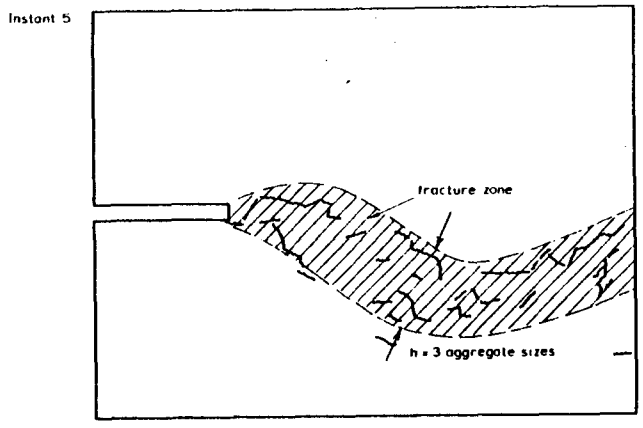

FIG. 8. Forces and Cracks as in Fig. 4 at Fifth Instant of Loading, Corresponding to Point 5 in Fig. 3(a)

the interface layer (Eq. 7) is taken as $f_t' = 355$ psi (1 psi = 6,895 Pa; 1 in. = 25.4 mm), and after the interface stress reaches the strength value, it instantly drops to zero.

Figs. 4–7 show the magnitudes of interparticle forces and the evolution of the system of microcracks as w is increased. The interparticle normal forces that exceed 80% of the strength limit of the contact, R_n^v, are drawn as the solid line segments; those which are > 60% but < 80% are drawn as the dashed line segments, and those which are > 40% but < 60% are drawn as the dotted line segments. The interface cracks are shown by the solid wavy line segments. Fig. 3(*a*) shows the diagram of vertical force resultant P of the reactions on the top boundary versus the top boundary displacement w. The secant dashed lines represent the current unloading diagrams of the system. These diagrams are straight and pass into the origin because no plastic dissipation is assumed to occur in the system. Otherwise, they would pass below the origin. Fig. 3(*b*) shows the total energy dissipation due to fracturing W^f as a function of top boundary displacement w. This energy is calculated by summing the energy dissipation over all the cracked interfaces. In each cracked interface, the energy dissipation is given by the area under the normal load-displacement diagram of the interface.

From Fig. 3(*a*), we see that after the cracking begins, the maximum load remains nearly constant for a few loading steps, then steeply declines at increasing displacement, and finally declines mildly toward a zero value. The short peak plateau, steep decline, and subsequent long tail of the load-deflection diagram are properties which well agree with various recent tests of tensile response of concrete in a stiff machine with fast servo-control involving a feedback from a displacement gage mounted over the cracking portion of the specimen; see Reinhardt and Cornelissen (1984), Wittmann (1983), van Mier (1984, 1986), and Bažant's review (1986). The energy dissipation [Fig. 3(*b*)] proceeds rapidly right after the peak load is reached but then advances very slowly with increasing displacement.

Figs. 4–8 show the states of interparticle forces and of cracking at various instants of loading, marked as 1,2,3,4, and 5 in Fig. 3(*a*). In Fig. 4, (instant 1), corresponding to the peak load at which the cracking just begins, we may notice the concentration of high forces near the notch and stress-free regions on the sides of the notch. In Fig. 5 (instant 2) the load is still about the same, but numerous cracks have formed, the region around the notch has been relieved from stress, and the heavily stressed region shifted forward. In Fig. 6 (instant 3), at which the load is reduced by about 40%, we see numerous discontinuous cracks forming ahead of the continuous crack, along with a partial relief of stress from various regions. At Fig. 7 (instant 4), the specimen still carries about 1/5 of the maximum load, although it is heavily cracked and nearly all uncracked interfaces are relieved from stress. Finally, Fig. 8 (instant 5), which corresponds to a state at which the displacement w is about six times the displacement at maximum load, shows the fracture process zone in the final stage of fracture. The boundaries of this zone, approximately marked by the solid curves, indicate that the width of the zone is approximately three times the maximum aggregate size. This agrees with the assumption made previously in the formulation of the crack band model (Bažant and Oh 1983). Note also that a single continuous crack has not yet formed at this large deformation.

As we see from Figs. 4–8, the present model yields quite a realistic picture of cracking in concrete. Since each individual aggregate piece must be modeled, the present model seems too complicated for large structures. It nevertheless appears to be adequate for studies of fracture regions of structures. Such studies have previously been carried out by finite elements; see, e.g., the works of Wittmann and Roelfstra (1984, 1985), in which each aggregate piece as well as the mortar matrix were subdivided by numerous finite elements, and crack formation between adjacent elements was analyzed. These previous approaches might be more realistic in their simulation of the microstructure; however, they require a vastly greater amount of computer time. The computer time requirements of such models would become particularly prohibitive in a generalization to three dimensions. A three-dimensional generalization of the present model, using, e.g., spherical rigid particles, would doubtless be much less demanding for computer memory and time.

On the other hand, the present limited study does not prove that exclusion of interface shear damage and frictional slip would be acceptable for all situations. Damage criteria involving a combination of normal and tangential interface forces might be required in other cases. Yet, the present formulation does not ignore such phenomena altogether; overall frictional resistance on some macroscopic slip plane is modeled by interface normal forces inclined with respect to this plane.

Conclusions

1. For the simulation of tensile fracture, brittle cementitious aggregate composites such as concrete may be modeled as a system of randomly arranged rigid particles interconnected by brittle interface layers. For the sake of simplicity, all deformations may be lumped into the center of each

interface layer, and the interface layer cracking may be based on a strength criterion for the normal interface force component.

2. The interface centers of each randomly generated particle need not lie on one circle, and thus the interfaces may define an irregularly shaped particle.

3. The model yields realistic load-displacement diagrams for fracturing specimens; it exhibits progressive softening, characterized by a steep initial decline followed by a long tail.

4. The simulation indicates that the width of the cracking zone (fracture process zone) is about three maximum aggregate sizes, which agrees with the assumption previously made in the blunt crack band model (Rodriguez-Ortiz 1974).

5. The fact that the model seems to yield realistic results confirms that the essential aspect of fracture should be the formation of discrete cracks in the thin interface layers of mortar between adjacent aggregate pieces. The detail of the distribution of microcracks throughout the matrix and the interface layers seems unimportant, as does the distribution of stresses throughout the aggregate pieces and the mortar matrix.

Acknowledgments

Partial financial support from the Air Force Office of Scientific Research under Contract No. F49620-87-C-0030DEF with Northwestern University, monitored by Dr. Spencer T. Wu, is gratefully acknowledged.

Appendix. References

Bažant, Z. P. (1984). "Imbricate continuum and its variational derivation." *J. Engrg. Mech.* ASCE, 110(12), 1693–1712.

Bažant, Z. P. (1985). "Fracture in concrete and reinforced concrete." *Mechanics of Geomaterials*, Z. P. Bažant, ed., John Wiley and Sons, New York, N.Y. 259–303.

Bažant, Z. P. (1986). "Mechanics of distributed cracking." *Appl. Mech. Rev.*, ASME, 4(5), 675–705.

Bažant, Z. P., Belytschko, T. B., and Chang, T. P. (1984). "Continuum theory for strain-softening." *J. Engrg. Mech.* ASCE, 110(12), 1666–1692.

Bažant, Z. P., and Chang, T. P. (1987). "Nonlocal finite element analysis of strain-softening solids." *J. Engrg. Mech.*, ASCE, 113(1), 89–105.

Bažant, Z. P., and Gambarova, P. (1980). "Rough cracks in reinforced concrete." *J. Struct. Div.*, ASCE, 106(ST3), 819–842.

Bažant, Z. P., and Oh, B. H. (1983). "Crack band theory for fracture of concrete." *Materials and Structures*, RILEM, Paris, France, 18(93), 155–177.

Cundall, P. A. (1971). "A computer model for simulating progressive large scale movements in blocky rock systems." *Proc. Int. Symp. on Rock Fracture*, ISRM, Nancy, France, 2–8.

Cundall, P. A. (1978). "BALL–A program to model granular media using the distinct element method." *Technical Note*, Advanced Technology Group, Dames and Moore, London, England.

Cundall, P. A., and Strack, O. D. L. (1979). "A discrete numerical model for granular assemblies." *Geotechnique*, 29, 47–65.

Gogate, A. B. (1980). Discussion of "Rough cracks in reinforced concrete," by Z. P. Gazant and P. Gambarova, *J. Struct. Div.*, 106(ST12), 2579–2581.

Kawai, T. (1980). "Some considerations on the finite element method." *Int. J. Numer. Meth. Engrg.*, 16, 81–120.

Palaniswany, R. G., and Shah, S. P. (1975). "A model for concrete subjected to triaxial stress." *Cem. Concr. Res.*, 5(4), 273–284.

Plesha, M. E., and Aifantis, E. C. (1983). "On the modeling of rocks with microstructure." *Proc. 24th U.S. Symp. on rock mechanics*, Texas A & M Univ., College Station, Tex., Jun., 27–35.

Reinhardt, H. W., and Cornelissen, H. A. W. (1984). "Post-peak cyclic behavior of concrete in uniaxial tensile and alternating tensile and compressive loading." *Cem. Concr. Res.*, 14(2), 263–270.

Rodriguez-Ortiz, J. M. (1974). "Study of behavior of granular heterogeneous media by means of analogical mathematical discontinuous models," (in Spanish), thesis presented to the Universidad Politecnica de Madrid, at Madrid, Spain, in partial fulfillment of the requirments for the degree of Doctor of Philosophy (in Spanish).

Serrano, A. A., and Rodriguez-Ortiz, J. M. (1973). "A contribution to the mechanics of heterogeneous granular media." *Proc., Symp. on Plasticity and Soil Mechanics*, Cambridge, U.K.

Shah, S. P., Chandra, S. (1968). "Critical stress, volume change, and microcracking of concrete." *J. Am. Concr. Inst.*, 5(9), 770–782.

Wittmann, F. H., ed. (1983). *Fracture mechanics of concrete*. Elsevier Publishing Co., Amsterdam, Netherlands, 321–324.

Wittmann, F. H., and Roelfstra, P. E., and Sadouki, H. (1984). "Simulation and analysis of composite structures." *Mat. Sci. and Engng.*, 68, 239–248.

Wittmann, F. H., and Roelfstra, P. E. (1985). "*Le béton numérique*." *Report*, EPFL, Lauanne; to appear in *Matériaux et Constructions*.

van Mier, J. G. M. (1984). "Strain softening of concrete under multiaxial loading conditions," thesis presented to the University of Eindhoven, at Eindhoven, the Netherlands, in partial fulfillment of the requirements for the degree of Doctor of Philosophy.

van Mier, J. G. M. (1986). "Multiaxial strain-softening of concrete." *Matériaux et Constructions*, RILEM, Paris, France, 19(111), 179–200.

Zubelewicz, A. (1980). "Contact elements method," thesis presented to the Technical University of Warsaw, at Warsaw, Poland, in partial fulfillment of the requirements for the degree of Doctor of Philosophy (in Polish).

Zubelewicz, A. (1983). "Proposal of a new structural model of concrete," *Archiwum Inzynierii Ladowej*, 29(4), 417–429, (in Polish).

Zubelewicz, A., and Mróz, Z. (1983). "Numerical simulation of rock-burst processes treated as problems of dynamic instability." *Rock Mech. and Engng.*, 16, 253–274.